Journal of
Plankton Research

academic.oup.com/plankt

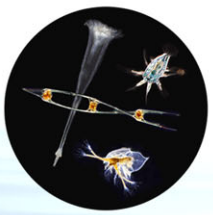

J. Plankton Res. (2017) 39(3): 531–549. *First published online February 25, 2017 doi:10.1093/plankt/fbx006*

Contribution to the Themed Section: Phytoplankton traits, functional groups and community organization

Phytoplankton diversity along spatial and temporal gradients in the Florida Keys

ELENA STANCA[1,2*,†] AND MICHAEL L. PARSONS[1]

[1]COASTAL WATERSHED INSTITUTE, FLORIDA GULF COAST UNIVERSITY, 10501 FGCU BLVD SOUTH, FORT MYERS, FL 33965, USA AND [2]DEPARTMENT OF BIOLOGICAL AND ENVIRONMENTAL SCIENCES AND TECHNOLOGIES, UNIVERSITY OF SALENTO, STRADA PROVINCIALE LECCE-MONTERONI, 73100 LECCE, ITALY

[†]PRESENT ADDRESS: DEPARTMENT OF BIOLOGICAL AND ENVIRONMENTAL SCIENCES AND TECHNOLOGIES, UNIVERSITY OF SALENTO, STRADA PROVINCIALE LECCE-MONTERONI, LECCE, ITALY

*CORRESPONDING AUTHOR: elena.stanca@unisalento.it

Received April 30, 2016; editorial decision January 31, 2017; accepted February 6, 2017

Corresponding editor: John Dolan

Environmental mechanisms that drive changes in phytoplankton community structure remain a remarkably understudied topic in phytoplankton ecology. For this study, two seasons and four sampling sites in the Florida Keys (FK) were selected for phytoplankton analyses to test if environmental constraints select for driving taxonomic diversity. One hundred and twenty-six taxa belonging to 10 classes and 6 phyla were identified, where significant differences in taxonomic composition and biovolume characterized the FK on spatial and temporal scales, with Bacillariophyta being the most representative phylum. A small number of taxa were limited to specific sites or seasons, whereas the majority were present at all sites and in both seasons, albeit in different densities. Canonical correspondence analysis results demonstrated that taxa are distributed along seasonal and spatial gradients defined by temperature, light and waves. The resultant variability in species composition indicates that the phytoplankton community structure is related to changing hydrodynamic conditions, temperature and light availability, which define the temporal and spatial filters for the most important phytoplankton functional groups observed in this study.

KEYWORDS: taxonomic/functional groups; diatoms; dinoflagellates; cyanobacteria; Florida Keys

INTRODUCTION

Phytoplankton are essential components of the global ecosystem (Field *et al.*, 1998; Falkowski *et al.*, 2004; Arrigo, 2005). Changes in their abundance and community structure can have profound impacts on higher trophic levels and key biogeochemical processes (Litchman *et al.*, 2007).

Additionally, changes in the composition and distribution of phytoplankton communities provide an excellent tool to interpret the dynamics of aquatic systems. Their small-scale responses to environmental variability justifies their use as sentinel organisms capable of detecting variations induced by climate change, increasing nutrient inputs, modifications in flow regimes and land use due to increasing anthropogenic pressure (Paerl and Huisman, 2009; Kruk *et al.*, 2011). It is important, therefore, to understand how these communities are structured, and to identify the drivers and mechanisms that can potentially shape phytoplankton composition.

The co-existence of phytoplankton assemblages under similar environmental conditions allows identification of functional groups made up of species with similar morphological, physiological and biochemical traits, or other defining characteristics (Iglesias-Rodríguez *et al.*, 2002; Pena, 2003; Le Quéré *et al.*, 2005; Alves-De Souza *et al.*, 2008; Roselli and Basset, 2015). Major taxonomic groups or Phyla, such as Bacillariophyta (diatoms), Dinophyta (dinoflagellates) and Cyanobacteria, are distinct functional groups, as these taxonomic groups have unique biogeochemical signatures and appear to differ in their parameters of nutrient uptake and growth, all of which translates into diverse ecological strategies (Litchman *et al.*, 2007). Therefore, the analysis of these major phytoplankton groups can be used to describe the global distribution of phytoplankton in aquatic ecosystems. In environments where vertical mixing energy is limited, motile phytoplankton are selectively favored because of their ability to access the resources needed for growth and survival, principally light and nutrients. For example, low tidal mixing energy is a factor that may contribute to the success of dinoflagellates, particularly during the summer when wind-mixing energy is at a minimum (Margalef, 1978, 1997; Smayda and Reynolds, 2001). In other environmental conditions, such as N-limited ecosystems, a number of dinoflagellate species also have a selective advantage (Harrison, 1976), owing in part to their ability to take up N at night (Paasche *et al.*, 1984), store significant amounts of N (Sciandra, 1991) and migrate through the water column in search of N sources (Olsson and Granelli, 1991). Additionally, some dinoflagellates can change their demand for nutrients through their trophic behavior, i.e. by utilizing mixotrophic feeding on smaller algae and bacteria.

On the other hand, the relatively high level of diatom dominance in regions that are well-mixed may in part be attributable to tidal mixing and wave energy. Diatoms are often more dependent on and tolerant of environments characterized by strong vertical mixing energy, while the turbulence of the water column in these situations may have a negative impact on the relative success of dinoflagellates (e.g. Wyatt and Horwood, 1973; Margalef, 1978; Margalef *et al.*, 1979; Smayda and Reynolds, 2001). Similarly, temperate winter and spring seasons and major upwelling conditions favor diatoms and often result in diatom blooms (Smayda and Reynolds, 2001). In general, planktonic diatoms seem well-adapted to regimes of intermittent light and nutrient exposure; additionally, they are particularly common in nutrient-rich regions encompassing polar as well as upwelling and coastal areas, highlighting their success in occupying a wide range of ecological niches and biomes (Malviyaa *et al.*, 2016).

In summary, dinoflagellates tend to behave as seasonal species, bloom soloists, are ecophysiologically diverse, and habitat specialists, whereas diatoms behave as perennial species, guild members, and are habitat cosmopolites. Diatoms have a relatively uniform bloom strategy based on species-rich pools and exhibit limited habitat specialization. Dinoflagellates have multiple life-form strategies consistent with their diverse habitat specializations, but rely on impoverished bloom species pools (Smayda and Reynolds, 2003).

Much of the research supporting the above statements was conducted in temperate and (sub)polar regions; much less work has taken place in the (sub)tropics. Would the same conclusions hold in these environments? In this study, we examined the phytoplankton composition and abundance across the various ecologically distinct regions of the Florida Keys (FK; USA), a region with a dearth of knowledge regarding phytoplankton composition and dynamics. The FK ecosystem is composed of tropical to subtropical waters that contain diverse community types, including bank reefs, patch reefs, hardbottom, seagrass beds and mangrove forests. The diversity of community types results in high species richness. It is one of the most ecologically diverse and most imperiled ecosystems in the USA, containing the third largest barrier coral reef ecosystem in the world. Upwelling of deep waters from internal tidal bores, current meanders and eddies provides a significant source of nutrients and storm events may also result in changes in circulation patterns that can allow nutrient enrichment (Zhang *et al.*, 2009; Nuttle and Fletcher, 2013). In addition, the geomorphology of the extensive shallow water areas surrounding the Keys, including numerous small mangrove islands found in these waters, reflect the influence of a stable regime of slowly rising sea level.

This study centered on the working hypothesis that taxonomic diversity is selected for by environmental and biotic constraints. Specifically, we hypothesized that distinct regions within the FK would exhibit different phytoplankton communities, and that these differences could be interpreted in terms of key distinguishing features of each region, including temperature and salinity variation, water energy, light intensity and the nutrient regime.

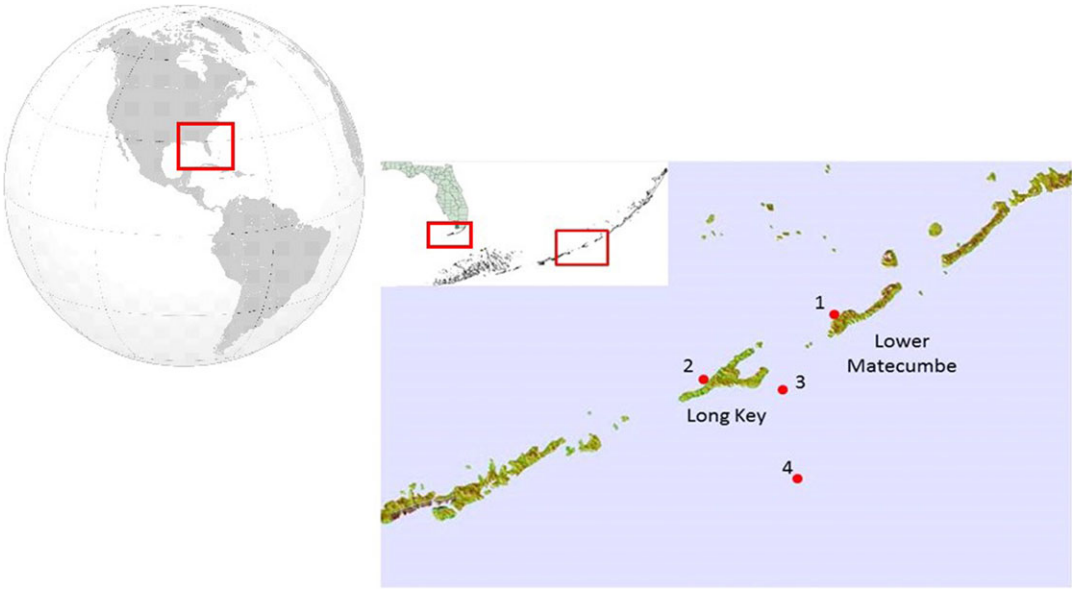

Fig. 1. Study area. (1) HGB on the bayside of Lower Matecumbe Key, (2) TPH on the bayside of Long Key, (3) LKH on the Atlantic side of Long Key and (4) TRL on Tennessee Reef.

METHOD

Study site description

The study utilized data collected from four locations in the vicinity of Long Key in the FK (Fig. 1). Two sites, Heine and Tomato Patch, are located in Florida Bay, and the other two, Long Key and Tennessee Reef, on the Atlantic Ocean side of the Keys. Heine (HGB) is a nearshore *Thalassia* seagrass bed, ~2 m deep. Siphonous chlorophytes are also present, including *Halimeda incrassata*, *Udotea* spp. and *Penicillis* spp. Tomato Patch (TPH) is a nearshore hardbottom site (~1.5 m in depth) consisting of soft corals, sponges and macroalgae, including *Laurencia gemmifera*, *Dictyota cervicornis* and *H. incrassata*. Long Key (LKH) is an offshore hardbottom site (~5 m in depth) consisting of soft corals, sponges and macroalgae, including *Laurencia intricata*, *D. cervicornis* and *Halimeda gracilis*. Tennessee Reef (TRL) is a barrier reef crest site (~7 m in depth) consisting of hard and soft corals, sponges and macroalgae, including turf algae, *Dictyota menstrualis* and *H. gracilis*. The ecotypes are heterogeneous both in terms of hydromorphic and physicochemical features. In addition to this water column heterogeneity, the benthos is also distinctive, due to the presence of different and particular macrophytes, such as *Dictyota*, *Thalassia* and *Halimeda*, which characterize each site.

Sampling field and laboratory methods

Water samples were collected in summer 2014 (June and July) and winter 2014–2015 (December and January) as part of the NOAA ECOHAB-funded CiguaHAB research project. A hierarchical sampling design was adopted for the integration of seasonal and spatial variations in phytoplankton community characteristics. Water samples were collected for phytoplankton using a van Dorn sampler within 0.5 m of the bottom. Three van Dorn samples were collected, each time the water being filtered through 200 and 20 μm sieves (15.3 cm diameter), for a total of 6.6 L of water collected and filtered. The material collected on the 20 μm sieve was then washed into a 50 mL centrifuge tube using ambient filtered seawater, and brought to a volume of 50 mL, and preserved with 1% glutaraldehyde (final volume).

At each station, abiotic water column parameters (bottom water temperature and benthic ambient light conditions) were recorded every 15 min using an Onset® HOBO® Pendant® Temperature/Light 64 K data logger (UA-002-64). The data loggers were retrieved and downloaded on a monthly basis. Salinity (surface and bottom) was measured using a refractometer when on-site for sampling. Wave data (simulated) were obtained from Wind Guru (http://windguru.cz/int/; GFS 27 km daily archive; Islamorada, FL) and corrected for fetch using wind data retrieved from the National Climatic Data Center (http://www.ncdc.noaa.gov) for the Marathon Airport (KMTH) using the Daily Summaries dataset. Wind corrections were applied as weights multiplied to the wave data, where winds coming from 10 to 40 degrees (NNE) were given weights of 0.5 (oceanside; TRL and LKH) and 0.25 (bayside; HGB and TPH); 50–230 degrees (NE–SW) were given weights of 1 (oceanside; TRL and LKH) and 0.1 (bayside; HGB and TPH) and

240–360 degrees (SW-N) were given weights of 1 (oceanside; TRL and LKH) and 0.5 (bayside; HGB and TPH). These factors down-weighted wave heights (in some cases) to acknowledge shorter fetch caused by the islands (primarily a factor for NE winds oceanside, and all but N-NW winds bayside), as well as the fact that waves are typically smaller bayside versus oceanside. As the wind-weights are hypothetical, the resulting wave heights were not directly comparable between sites and were therefore limited to within-site analyses. Temperature, light and wave data were averaged to daily values, and then averaged at 3-day, 1-week, 2-week and 1-month intervals prior to sampling to account for immediate (1 day), short-term (3 day and 1 week) and long-term (2 weeks and 1 month) influences of these variables on planktonic populations.

Water samples for nutrient analysis were collected in triplicate at each site within 0.5 m of the bottom in acid-washed, 250 mL PFTE bottles. Back on shore, the samples were filtered through acid-washed, Whatman GF/F glass fiber filters (0.7 μm nominal pore size), into clean 250 mL glass amber bottles and frozen until analyzed. Nutrient concentrations (nitrate, nitrite, ammonium and phosphate) were determined in accordance with standard laboratory methods on a Bran+Luebbe AutoAnalyzer 3.

Phytoplankton analysis

General microalgae composition was determined by transferring 3 mL of phytoplankton sample into one well of a 6-well flat-bottomed tissue culture plate (Corning™ Costar™), left to settle for several hours, and thereafter analyzed on an Olympus IX71 phase contrast inverted microscope using magnification of ×200 and ×400. A minimum of 400 phytoplankton cells per sample were identified to the lowest taxonomic level possible. Light microscopy was aided by other techniques to confirm the identification of certain key dinoflagellates and diatoms, including epifluorescence microscopy using Uvitex® staining (similar to calcofluor; Polysciences, Ltd, cat. #19 517-10; for armored dinoflagellates) and acid-digestion of samples followed by analysis using differential interference contrast microscopy (diatoms). While glutaraldehyde preservation can hinder phytoflagellate identification in general, we identified and classified such cells whenever possible based on specific morphological traits (such as shape, size, etc., of some Chlorophyta, Pyramimonadophyceae). In cases where such classification was not possible, we categorized the cells as "phytoflagellate undetermined". Similarly, other groups that could not be identified to lower taxonomic units were also classified as "undetermined" (e.g. Dinophyceae thecate undetermined).

The texts and journal articles used most frequently to aid in taxonomic identification were: Cupp (1977), Patrick and Reimer (1966), Dodge (1982), Foged (1984), Sournia (1986), Tomas (1997), Witkowski *et al.* (Witkowski *et al.*, 2000), Faust and Gullendge (2002), Trobajo Pujadas (2007), Hein *et al.* (Hein *et al.*, 2008), Al-Kandari *et al.* (Al-Kandari *et al.*, 2009), Lobban and Schefter (2012) and Hoppenrath *et al.* (Hoppenrath *et al.*, 2014).

Cell biovolumes were estimated by assigning combinations of geometric shapes to fit the characteristics of individual taxa and were calculated for each cell, according to the specimen/genus/class-specific shape association (Hillebrand *et al.*, 1999; Sun and Liu, 2003; Vadrucci *et al.*, 2007) and using the formulas recorded in "Atlas of shape" (http://phytobioimaging.unisalento.it/en-us/products/AtlasOfShapes.aspx?ID_Tipo = 0). Specific cell dimensions were measured for each phytoplankton cell to calculate biovolume. Total biovolume per sample ($\mu m^3\ L^{-1}$ for phytoplankton) was calculated by multiplying cell biovolume (μm^3) by its corresponding abundance (cells L^{-1}) for each species.

Statistical analyses

Only those phytoplankton present in ≥25% of the water samples were analyzed in order to reduce the influence of infrequently occurring taxa on the subsequent analysis (Clarke and Gorley, 2015). An analysis of similarities (two-way crossed ANOSIM; Clarke, 1993) was used to compare the taxonomic composition between ecotype and seasons. The comparison was based on Bray–Curtis similarity values (Bray and Curtis, 1957) of the common taxa present in each sample. Data were (ln + 1) transformed prior to analysis.

The differences between ecotype and seasons were examined using non-parametric multi-dimensional scaling ordination (nMDS). For this analysis, ecotype centroids were determined, which are defined as the mean values for each taxon in each ecotype and season. In the nMDS plot, the stress value indicates the goodness of representation of differences among ecotype centroids. SIMPER (Similarity Percentage; Clarke, 1993) was used to determine how typical each species was of each ecosystem. In this case, sampling points were again used as replicates. ANOSIM, nMDS and SIMPER were all computed using PRIMER 7 software (PRIMER-E Ltd).

Canonical correspondence analysis (CCA) was performed by multivariate ordination using CANOCO version 4.0 following Ter Braak (1986), to examine the relationship between physical/chemical parameters and the structure of the phytoplankton assemblage. For this analysis, a matrix was built containing the physical and chemical parameters versus the total biomass of each phytoplankton species ($\mu m^3\ L^{-1}$) in each sample. Physical and chemical data were centered about the mean of the

Table I: Environmental physico-chemical characteristics during study period (Winter and Summer seasons) at the four stations studied

	Winter				Summer			
Parameter	HGB	LKH	TPH	TRL	HGB	LKH	TPH	TRL
3dT (C)	21.34 (19.78–22.91)	23.63 (23.33–23.91)	23.21 (22.89–23.40)	24.63 (24.21–25.07)	31.19 (30.55–31.84)	29.61 (28.10–31.10)	30.01 (28.52–31.52)	29.11 (27.98–30.24)
3dwave (m)	0.15 (0.13–0.17)	0.41 (0.34–0.48)	0.22 (0.17–0.30)	0.41 (0.34–0.48)	0.04 (0.02–0.06)	0.25 (0.15–0.36)	0.04 (0.02–0.06)	0.25 (0.15–0.35)
3dL (µE)	65.80 (60.00–71.60)	42.34 (42.03–42.64)	136.26 (78.99–193.53)	52.05 (46.10–58.00)	217.16 (215.83–218.48)	139.39 (120.08–124.39)	120.65 (116.90–124.39)	87.28 (67.48–107.09)
Ammonium (µM)	1.658 (1.417–1.900)	0.677 (0.630–0.723)	0.827 (0.792–0.862)	0.484 (0.482–0.487)	2.939 (2.648–3.230)	1.169 (1.006–1.332)	2.651 (2.122–3.180)	1.131 (0.747–1.514)
Nitrate (µM)	0.136 (0.029–0.244)	0.127 (0.022–0.232)	0.083 (0.060–0.106)	0.022 (0.022–0.022)	0.022 (0.022–0.022)	0.101 (0.022–0.181)	0.155 (0.087–0.222)	0.022 (0.022–0.022)
Nitrite (µM)	0.013 (0.005–0.021)	0.017 (0.003–0.031)	0.003 (0.003–0.003)	0.003 (0.003–0.003)	0.003 (0.003–0.003)	0.003 (0.003–0.003)	0.008 (0.003–0.014)	0.008 (0.003–0.014)
Phosphate (µM)	0.130 (0.122–0.137)	0.123 (0.110–0.135)	0.128 (0.126–0.130)	0.134 (0.114–0.154)	0.230 (0.066–0.394)	0.045 (0.031–0.059)	0.087 (0.072–0.102)	0.052 (0.034–0.071)

variable and reduced by the variance. CCA is an efficient ordination technique when a Gaussian relationship between species and the environmental gradients is expected (Ter Braak, 1986). This constrained analysis extracts the best environmental gradients that explain the maximum variability in species data. Initially, 18 chemical and physical parameters were input into the CCA. Forward selection was used to identify the most significant subset of environmental variables ($P \leq 0.05$). The significance of the first axis and of all axes was analyzed using the Monte Carlo test, under unrestricted model of 999 permutations ($P \leq 0.01$). Environmental data were also transformed as needed ($\log(x + 1)$) or square-root transformed to satisfy the assumption of normality and homogeneity of variance.

RESULTS

Physical and chemical parameters

An evaluation of the overall site means of physical and chemical parameters is presented in Table I. The data collected during four sampling periods, June, July, December and January, were designated as Summer and Winter, respectively. In general, temperatures were lower in Winter (HGB: 21.34°C; TPH: 23.21°C) than in Summer (HGB: 31.19°C; TPH: 30.01°C). A regional and temporal fluctuation was observed in wave height. During Winter, the wave heights varied between 0.15 (HGB) and 0.41 m (LKH and TRL). During Summer, wave heights were lower on average, with a minimum of 0.04 (HGB and TPH) and a maximum of 0.25 m (LKH and TRL). Lastly, average light intensity (µE) was lower in Winter (LKH: 42.34; TRL: 52.05) than in Summer (TRL: 87.28; TPH: 120.65). The seasonal trends are confirmed when examining the monthly values of these parameters for each site (Fig. 2). Wave heights are higher in the Winter versus Summer, whereas temperature and light values are lower.

Nutrient concentrations were very low, and did not vary significantly at spatial or temporal scales. The average concentrations of ammonium ranged from 0.49 µM (TRL) to 1.66 µM (HGB) in Winter. Higher values were reported in Summer, varying from 1.13 µM (TRL) to 2.94 µM (HGB). The average concentrations of nitrate ranged from 0.02 µM (TRL) to 0.14 µM (HGB) in Winter and from 0.02 µM (HGB, TRL) to 0.16 µM (TPH) in Summer. The average concentrations of nitrite ranged from 0.003 µM (TPH, TRL) to 0.17 µM (LKH) in Winter and from 0.003 µM (HGB, LKH) to 0.008 µM (TPH, TRL) in Summer. The average concentrations of phosphate ranged from 0.12 µM (LKH) to 0.13 µM (TRL) in Winter and from 0.04 µM (LKH) to 0.23 µM

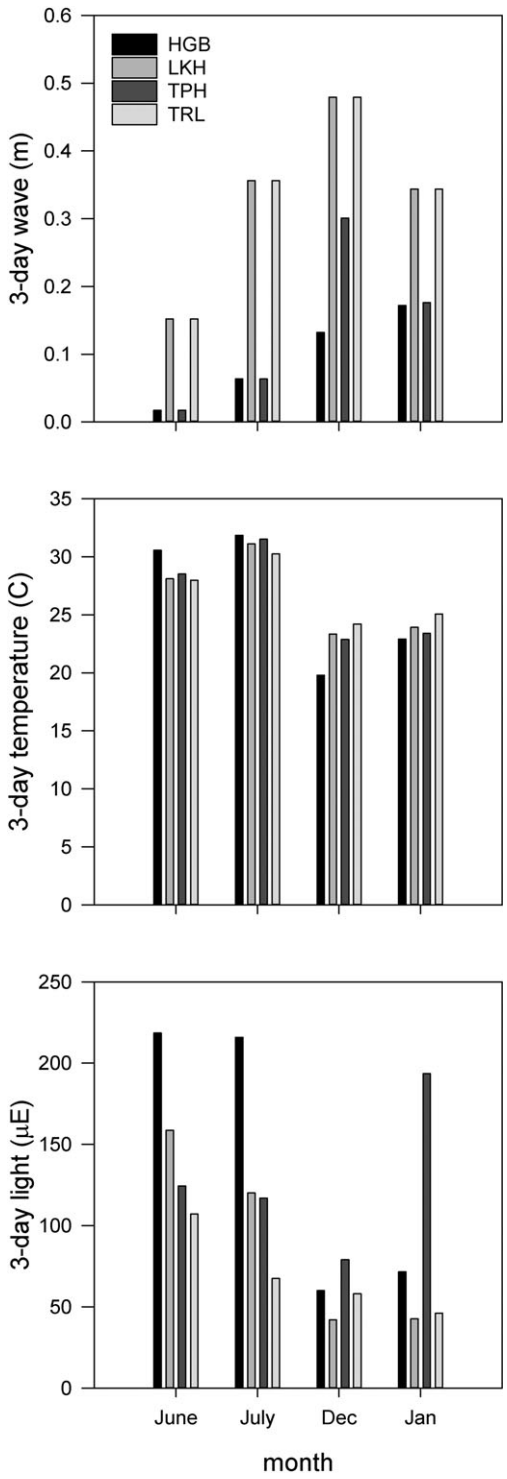

Fig. 2. Monthly physical characteristics at the four stations studied: HGB, TPH, LKH and TRL.

(HGB) in Summer. Visual inspection of the nutrient data on a monthly basis indicates that seasonal differences are not strongly evident (Fig. 3). For example, nitrate was generally highest in July and December and phosphate exhibited the highest site value in July (HGB), although concentrations were higher at the other sites in winter months. Nitrite was generally extremely low except for higher concentration recorded each month at different sites. Ammonium provided the clearest example of seasonal differences, with concentrations generally being higher in the summer versus winter months.

Phytoplankton composition and distribution

Overall, 6400 phytoplankton cells were counted, measured and classified. A total of 126 taxa were identified, belonging to 6 Phyla (major taxonomic/functional group) and 10 Classes. Over 59% of the taxa were Bacillariophyta; among the remaining taxa, 30% were Dinophyta, 7% were Cyanobacteria, ~2% were Chlorophyta and <1% were Cryptophyta and Other Phytoplankton. Specifically, recorded taxa were classified as follows: 75 diatoms (23 Bacillariophyceae, 20 Fragilariophyceae, 24 Mediophyceae, 8 Coscinodiscophyceae), 38 Dinophyceae, 9 Cyanophyceae, 2 Chlorophyceae, 1 Trebouxiophyceae, 1 Cryptophyceae, 1 Pyramimonadophyceae and 1 Other Phytoplankton. Of the 48 common taxa used in subsequent analysis, 65% were Bacillariophyta, with the remainder composed of Cyanobacteria (10%) and Dinophyta (21%). Cryptophyta and Other Phytoplankton were the less representative phyla accounting for 2% of the overall composition.

Total biovolume and morphological traits of these 48 taxa are presented in Table II. *Thalassiophysa hyalina* was the most dominant diatom taxon, representing 16% of total biovolume; *Oscillatoria* spp. was the most representative Cyanobacteria taxa (11%); Dinophyceae thecate undetermined was the main taxon component of the Dinophyta (15%); Cryptophyceae undetermined and Phytoflagellates undetermined (with total biovolume <1%) were most dominant for Cryptophyta and Other Phytoplankton, respectively.

Mean cell size (μm^3 ± SE) ranged from 102.73 ± 2.47 for Phytoflagellates undetermined to 327 090.61 ± 69 478.56 for the diatom, *Climacosphenia moniligera*. Among the Bacillariophyta, mean cell size (μm^3 ± SE) ranged from 372.42 ± 10.04 for *Ceratoneis closterium* to 327 090.61 ± 69 478.56 for *C. moniligera*. Cyanobacteria cell sizes had a narrower range, from 43 399.79 ± 4449.84 for *Gomphosphaeria aponina* to 1136.76 ± 83.37 for Cyanophyceae undetermined 2f, as did Dinophyta, ranging from 8951.47 ± 288.32 for *Tripos furca* to 195 305.63 ± 45 357.94 for *Gambierdiscus* spp. Overall phyla-level biovolume values (±SE) ranged from 22 766.41 ± 959.38 for Dinophyta, followed by Cyanobacteria (20 014.33 ± 1142.10) and Bacillariophyta (11 098.81 ± 794.20).

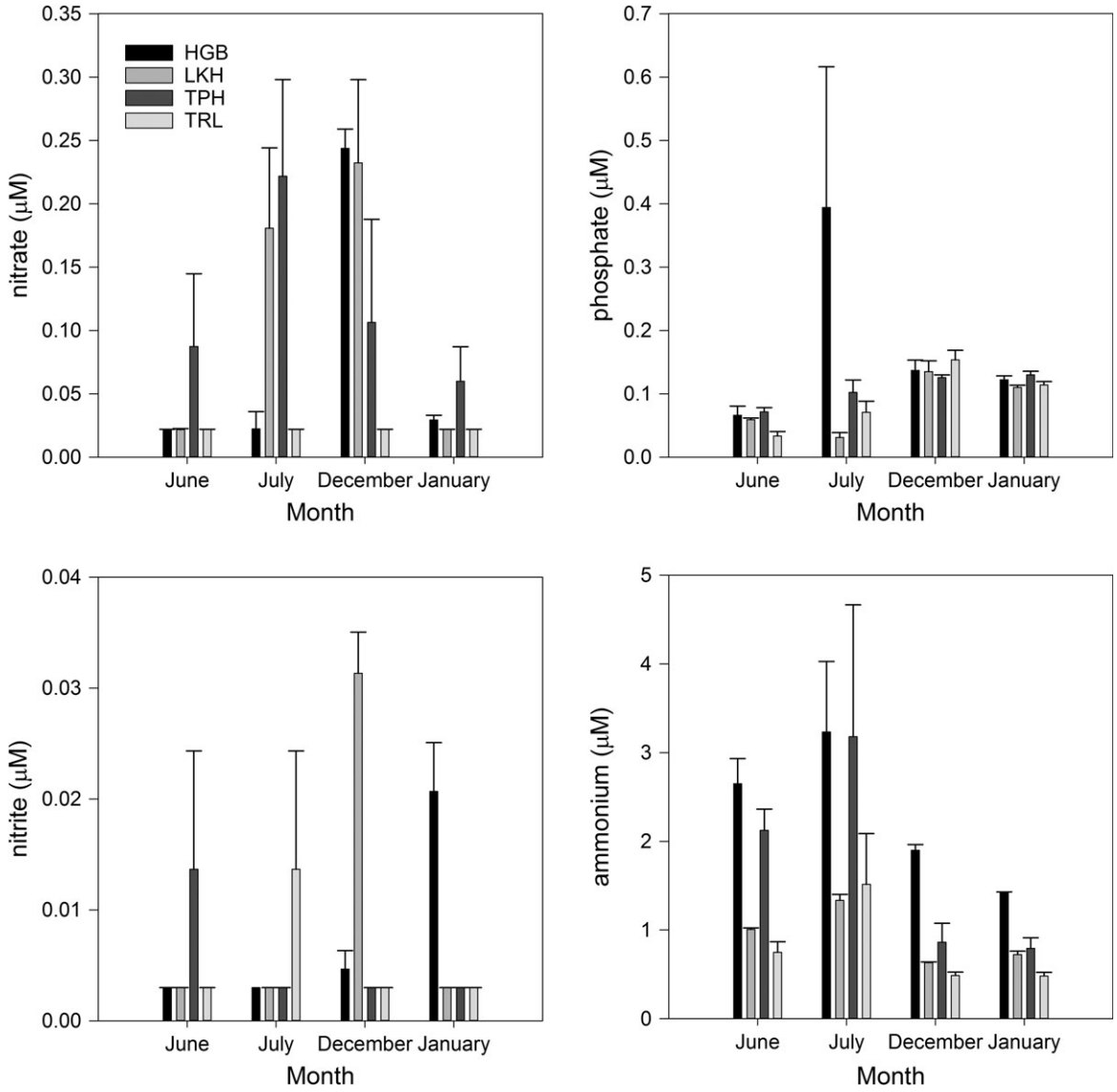

Fig. 3. Monthly nutrient concentrations at the four stations studied: HGB, TPH, LKH and TRL.

While Bacillariophyta was generally the most representative phylum, there was high compositional variability in total biovolume among the different phyla on spatial and temporal scales. Spatially, Bacillariophyta total biovolume was highest at TRL (79%), whereas Dinophyta was highest at LKH (33%) and Cyanobacteria at TPH (27%). The lowest values were observed for Cryptophyta at HGB (0.01%), LKH (0.04%), TPH (0.06%) and TRL (0.31%) (Fig. 4a). Seasonally, Bacillariophyta total biovolume was highest in the winter (73%), while Dinophyta (28%) and Cyanobacteria (18%) were most abundant in the summer (Fig. 4b). The lowest values were observed for Cryptophyta in summer (<1%).

Spatially, Cyanobacteria cells were the largest (on average) observed at HGB (29 685.89 ± 3064.59 μm^3), whereas Dinophyta had the largest cells at the other three sites, varying from a maximum value at TRL (29 206.47 ± 12 034.64 μm^3) to a minimum value at TPH (22 454.17 ± 1409.67 μm^3) (Fig. 5a). Seasonally, Dinophyta cells were biggest during winter (32 434.42 ± 4630.76 μm^3), and Cyanobacteria were biggest during summer (26 155.16 ± 1262.02 μm^3) (Fig. 5b).

In summary, phytoplankton communities were dominated by Bacillariophyta at all sites across seasons. Dinophyta and Cyanobacteria contributed biovolumetrically by having the largest average cell sizes on both spatial (HGB—Cyanobacteria; the other three sites—Dinophyta) and temporal scales (summer—Cyanobacteria; winter—Dinophyta).

Table II: List of six major taxonomic/functional group, total biomass (total biovolume $\mu m^3 L^{-1}$), mean ± standard error for organism size (μm^3) of phytoplankton taxa collectively accounting for 25% of the total number of samples examined

Phyla	Taxa	Mean organism size μm^3 ± E.S.	Total biovolume $\mu m^3 L^{-1}$	Shape typology	Shape code	Taxa code
Ba	*Bleakeleya notata* (Grunow) Round	47 322.36 ± 5473.00	12 085 692.40	C-elo	21	Blea
Ba	*Ceratoneis closterium* Ehrenberg 1839	372.42 ± 10.04	741 889.30	C-elo	16	Cera
Ba	*Chaetoceros curvisetus* Cleve 1889	3451.61 ± 341.14	1 541 483.02	S-elo	8	Chcu
Ba	*Chaetoceros decipiens* Cleve 1873	12 122.81 ± 1388.74	4 445 568.01	S-elo	8	Chde
Ba	*Chaetoceros laciniosus* F. Schütt 1895	3729.95 ± 395.89	2 386 098.11	S-elo	8	Chla
Ba	*Chaetoceros laevis* G. Leuduger-Fortmorel 1892	737.25 ± 63.16	944 226.41	S-elo	8	Chle
Ba	*Chaetoceros wighamii* Brightwell 1856	1074.69 ± 101.84	2 276 991.08	S-elo	8	Chwi
Ba	*Chaetoceros* spp.	2891.12 ± 162.21	13 597 942.05	S-elo	8	Chsp
Ba	*Climacosphenia moniligera* Ehrenberg	327 090.61 ± 69 478.56	10 583 089.45	C-elo	21	Clim
Ba	*Coscinodiscus* spp.	221 989.19 ± 42 636.22	21 911 922.19	S-elo	3	Cosc
Ba	*Cyclotella* spp.	5795.38 ± 390.73	7 192 434.68	S-elo	3	Cycl
Ba	*Entomoneis alata* (Ehrenberg) Ehrenberg 1845	109 401.41 ± 27 025.27	12 020 892.70	S-elo	8	Ento
Ba	*Eunotia* cf. *lunaris*	1042.91 ± 78.82	130 727.42	S-elo	41	Euno
Ba	*Hemiaulus hauckii* Grunow ex Van Heurck 1882	18 940.72 ± 3295.12	830 478.42	S-elo	8	Hemi
Ba	*Licmophora flabellata* (Grev.) C. Agardh 1831	23 688.79 ± 4758.57	2 634 617.54	S-elo	40	Lifl
Ba	*Licmophora remulus* Grunow 1867	13 525.09 ± 2582.08	2 419 549.38	S-elo	40	Lire
Ba	*Licmophora* spp.	19 441.39 ± 3330.98	7 681 766.44	S-elo	40	Lisp
Ba	*Mastogloia fimbriata* (T. Brightwell) Grunow 1863	27 079.42 ± 2268.62	2 657 288.82	S-elo	8	Mast
Ba	*Microtabella interrupta* (Ehrenberg) Round 1990	17 126.37 ± 2434.17	8 901 134.85	S-elo	8	Micr
Ba	*Navicula* spp.	628.62 ± 12.44	4 180 922.21	S-elo	8	Nasp
Ba	*Navicula transitans* Cleve 1883	1073.96 ± 87.14	465 375.93	S-elo	8	Natr
Ba	*Pleurosigma* spp.	1553.14 ± 258.69	64 536.81	S-elo	9	Pleu
Ba	*Rhabdonema adriaticum* Kützing 1844	105 062.83 ± 28 783.44	15 262 935.17	S-elo	7	Rhab
Ba	*Striatella unipunctata* (Lyngbye) C. Agardh 1832	24 951.94 ± 8650.51	1 677 660.62	S-elo	8	Stri
Ba	*Synedra* cf. *fulgens* var. *gigantea*	62 986.93 ± 9422.38	7 405 513.06	C-elo	48	Syfu
Ba	*Synedra crotonensis* var. *prolongata* Grunow 1881	15 187.63 ± 1398.91	12 194 619.10	C-elo	48	Sycr
Ba	*Synedra* spp.	134 794.61 ± 35 864.66	9 252 255.24	S-elo	7	Sysp
Ba	*Tabellaria* cf. *fenestrata*	21 013.70 ± 2870.47	6 924 579.53	S-elo	7	Tabe
Ba	*Thalassionema* spp.	6229.22 ± 879.03	1 914 187.03	S-elo	7	Thal
Ba	*Thalassiophysa hyalina* (Greville) Paddock & P.A. Sims 1981	139 621.35 ± 17 691.92	66 327 614.77	S-elo	8	Thhy
Ba	*Toxarium undulatum* J.W. Bailey 1854	64 146.22 ± 19 285.31	2 738 714.83	C-elo	48	Toxa
Cr	Cryptophyceae undet.	445.17 ± 12.36	263 034.61	C-glo	19	Cryp
Cy	*Anabaena* spp.	29 599.69 ± 12 938.78	3 059 124.84	S-elo	3	Anab
Cy	*Gomphosphaeria aponina* Kützing	43 399.79 ± 4449.84	7 513 313.98	S-sph	1	Gomp
Cy	*Oscillatoria* spp.	26 486.11 ± 1123.18	44 627 005.87	S-elo	3	Osci
Cy	Cyanophyceae undet.	8528.93 ± 2704.96	1 496 870.61	S-elo	3	Cyun
Cy	Cyanophyceae undet. 2f	1136.76 ± 83.37	503 594.81	S-elo	3	Cy2f
Di	*Coolia* spp.	19 782.53 ± 368.51	6 913 577.15	S-glo	4	Cool
Di	*Gambierdiscus* spp.	195 305.63 ± 45 357.94	7 188 857.82	S-glo	4	Gamb
Di	*Gonyaulax* spp.	20 813.05 ± 1969.74	2 225 922.73	C-glo	14	Gony
Di	*Ostreopsis* cf. *heptagona*	65 903.72 ± 9136.55	9 960 894.67	S-glo	4	Ostr
Di	*Prorocentrum belizeanum* M.A .Faust 1993	21 335.47 ± 561.31	3 724 582.40	S-glo	4	Prbe
Di	*Prorocentrum lima* (Ehrenberg) F. Stein 1878	21 513.91 ± 4649.68	854 660.75	S-glo	4	Prli
Di	*Protoperidinium* spp.	13 345.35 ± 712.38	4 814 720.16	C-glo	14	Prot
Di	*Scrippsiella* spp.	9288.63 ± 2157.29	421 925.99	S-glo	4	Scri
Di	*Tripos furca* (Ehrenberg) Vanhoeffen 1897	8951.47 ± 288.32	10 509 667.30	C-glo	23	Bice
Di	Dinophyceae thecate undet. 1 (> 20 μm)	26 635.56 ± 561.38	61 485 777.27	S-glo	1	Dino
Ot	Phytoflagellates undet.	102.73 ± 2.47	1 790 071.92	S-glo	1	Phyt

Ba = Bacillariophyta; Ch = Chlorophyta; Cr = Cryptophyta; Cy = Cyanobacteria; Di = Dinophyta; Ot = Other Phytoplankton; C = complex shape; S = simple shape; elo = elongated; glo = globular; sph = sphaerical; 1 = Sphere; 3 = Cylinder; 4 = Ellipsoid; 7 = Parallelepiped; 8 = Prism on elliptic base; 9 = Prism on parallelogram base; 14 = Double cone; 16 = Prolate spheroid + 2 cylinder; 19 = Cone + half sphere; 21 = Prism on elliptic base + parallelepiped; 23 = Ellipsoid + 2 cones + cylinder; 40 = Gomphonemoid; 41 = Sickle-shaped prism; 48 = 2 Parallelepiped + elliptic prism.

Dynamics of discriminating phytoplankton taxa

Overall, the taxonomic composition of the phytoplankton community varied significantly among sites and seasons (one-way ANOSIM, Global R (site) = 0.214, $P < 0.042$; Global R (season) = 0.548; $P < 0.001$). The nMDS ordination diagram arranged the study sites into two groups (Fig. 6a), according to their geographic region (open ocean—O; and coastal bay—B). The first group (O) included the TRL and LKH and the second one HGB

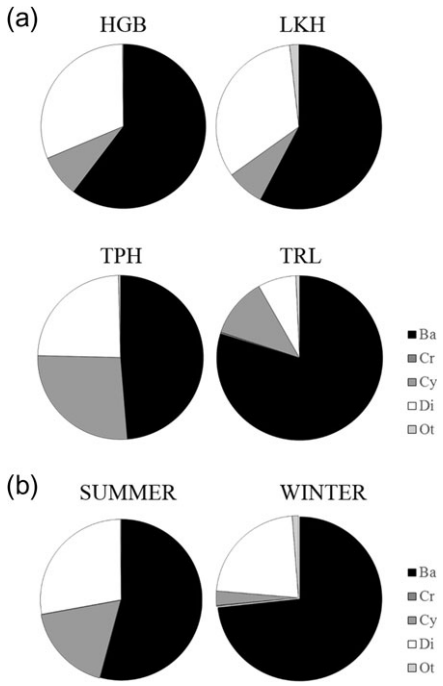

Fig. 4. Total biovolume distribution among taxonomic classical functional groups, at (**a**) spatial and (**b**) temporal scales. Station abbreviations are defined in Table I. Taxonomic abbreviations are defined in Table II.

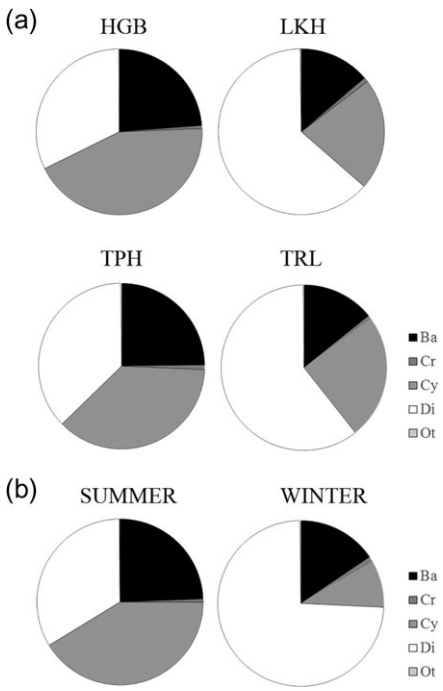

Fig. 5. Biovolume distribution among taxonomic classical functional groups, at spatial and temporal scales. Station abbreviations are defined in Table I. Taxonomic abbreviations are defined in Table II.

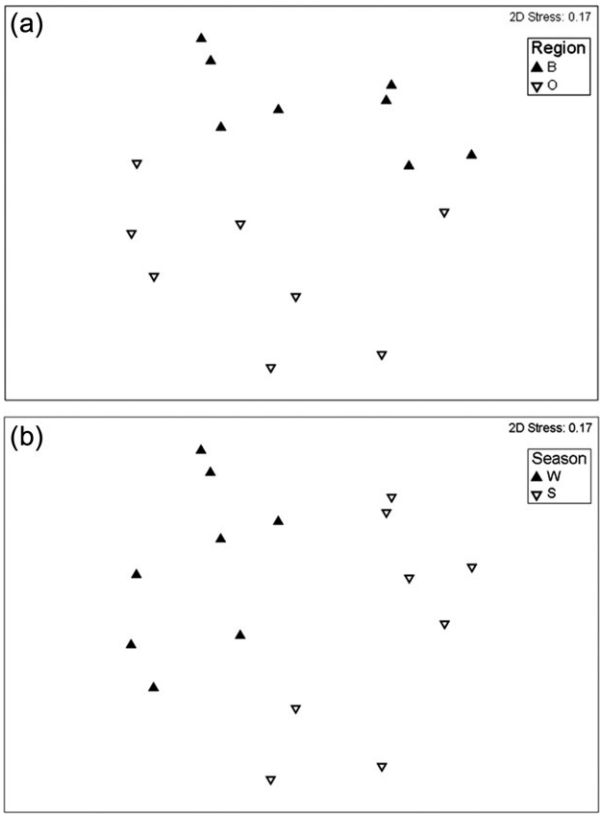

Fig. 6. nMDS of ecosystem centroids of phytoplankton total biovolume per taxon for each (**a**) spatial (O, Ocean; B, Bay) and (**b**) seasonal period (W, Winter; S, Summer).

and TPH (B), respectively. Similarly, the samples separated into two seasonal groups as well (Fig. 6b).

SIMPER analysis ranked taxa in terms of how each contributed to the dissimilarity (up to 70% dissimilarity) between all pairs of intergroup samples at the regional (spatial) and seasonal level (Tables III and IV). There were 28 taxa in total that constituted the 70% dissimilarity threshold, 23 of which were common at spatial and temporal scales. In particular, four Bacillariophyta and one Dinophyta were the most influential taxa that associated with dissimilarity on the spatial scale (see Table III), whereas three Bacillariophyta, two Dinophyta and two Cyanobacteria characterized the seasonal differences (see Table IV). Spatially, only two taxa were both present at the oceanside sites and absent at the bayside sites (*Chaetoceros decipiens* and *Hemiaulus hauckii*; Bacillariophyta), and only one, *Prorocentrum lima* (Dinophyta), was present at the bayside sites and absent at the oceanside sites. The remaining taxa were present in both regions, but 21 taxa were more abundant bayside. This spatial distribution was most probably due to the influence of different hydrodynamic and physico-chemical conditions that determined

Table III: The results of the SIMPER (similarity percentage) analysis displaying the average total biovolume (Tbiov) of the most abundant phytoplankton taxa (contributing at least 1% of the difference) differentiating Bayside phytoplankton from Oceanside phytoplankton

Taxa	Average bayside Tbiov	Average oceanside Tbiov	Average dissimilarity	% contribution	Cumulative %
Chaetoceros decipiens Cleve 1873	0	11.35	1.99	3.91	3.91
Rhabdonema adriaticum Kützing 1844	10.36	1.67	1.65	3.25	7.16
Licmophora spp.	10.79	3.03	1.56	3.07	10.23
Prorocentrum belizeanum MA Faust 1993	9.78	2.91	1.47	2.9	13.12
Entomoneis alata (Ehrenberg) Ehrenberg 1845	10.48	4.97	1.42	2.8	15.92
Ostreopsis cf. *heptagona*	8.71	3.21	1.4	2.76	18.68
Synedra spp.	8.64	3.08	1.36	2.67	21.35
Dinophyceae thecate undet. 1 (> 20μm)	9.66	8.43	1.36	2.67	24.02
Mastogloia fimbriata (T. Brightwell) Grunow 1863	8.15	1.36	1.34	2.64	26.66
Coscinodiscus spp.	7.69	1.81	1.32	2.6	29.26
Microtabella interrupta (Ehrenberg) Round 1990	13.36	5.92	1.32	2.59	31.85
Gonyaulax spp.	7.84	1.34	1.31	2.57	34.42
Anabaena spp.	7.8	1.45	1.3	2.56	36.98
Oscillatoria spp.	5.57	6.69	1.29	2.53	39.51
Chaetoceros laevis G. Leuduger-Fortmorel 1892	2.61	8.19	1.25	2.46	41.97
Bleakeleya notata (Grunow) Round	3.42	7.21	1.24	2.45	44.41
Synedra cf. *fulgens* var. *gigantean*	6.98	4.91	1.24	2.44	46.85
Coolia spp.	6.75	4.55	1.2	2.37	49.22
Gomphosphaeria aponina Kützing	6.96	3.06	1.2	2.36	51.57
Protoperidinium spp.	6.82	4.34	1.18	2.32	53.9
Thalassionema spp.	7.5	4.52	1.14	2.25	56.14
Thalassiophysa hyalina (Grev.) Paddock & P.A. Sims 1981	6.02	1.66	1.08	2.13	58.28
Gambierdiscus spp.	5.22	3.59	1.07	2.11	60.39
Prorocentrum lima (Ehrenberg) F. Stein 1878	6.07	0	1.06	2.09	62.48
Hemiaulus hauckii Grunow ex Van Heurck 1882	0	6.09	1.04	2.04	64.52
Climacosphenia moniligera Ehrenberg	1.8	5.5	1.02	2.01	66.53
Chaetoceros laciniosus F. Schütt 1895	0.93	5.78	1.02	2.01	68.54
Licmophora flabellata (Grev.) C. Agardh 1831	4.96	3.05	1.01	2	70.53

The total biovolume values are given as ln ($\mu m^3 L^{-1}$ + 1). The average dissimilarity is based on Bray–Curtis similarity and is computed by calculating the dissimilarity between Bayside sites (HGB and TPH) and the Oceanside sites (LKH and TRL). The % contribution values indicate how much each taxon contributes to the overall dissimilarities between the two regions, with the cumulative % value summing these values to demonstrate how the overall dissimilarity is built by the contributing species.

the success of these taxa in the bayside sites over the oceanside sites.

Seasonally, only four taxa were present during summer and absent during winter (*G. aponina*, *Coscinodiscus* spp., *T. hyalina* and *Cyclotella* spp.; belonging to Cyanobacteria and Bacillariophyta, respectively), and only one, *Navicula transitans* (Bacillariophyta), was present during winter and absent during summer. The other 23 taxa were common at all sites during winter and summer seasons, but in different abundances. Particularly, 50% of taxa were more common in the winter, and 50% more so in the summer (Table IV), similar to the classical seasonal succession of phytoplankton, but different in that some diatoms were more common during summer, and some dinoflagellates more so during winter. These findings suggest that spatial and temporal assemblage differences are characterized primarily by few taxa, and that the changes in the abundance of common species are driven by other abiotic factors.

Phytoplankton assemblage dynamics

We used CCA to link the variability in the structure of phytoplankton assemblage to physical and chemical parameters (Fig. 7a–d). The length of the environmental variable arrows in the ordination diagram in Fig. 7 represents the relative importance of each variable in relation to the taxa.

After the forward selection procedure, the CCA analysis revealed that three environmental variables [3-day temperature (3dT), 3-day wave (3dw) and 3-day light (3dL)] made significant contributions ($P < 0.001$) to the variance, providing a good representation of the major environmental factors relating to phytoplankton structure. The eigenvalues of the first two canonical axes (0.18 and 0.11, respectively) explained 32% of the total variance. The phytoplankton species and environmental variables showed correlation values of 0.93 and 0.90 on canonical axes 1 and 2, respectively, suggesting a strong relationship between the three environmental variables

Table IV: The results of a SIMPER (similarity percentage) analysis displaying the average total biovolume of the most abundant phytoplankton taxa (contributing at least 1% of the difference) differentiating Winter phytoplankton from Summer phytoplankton

Taxa	Average winter Tbiov	Average summer Tbiov	Average dissimilarity	% contribution	Cumulative %
Dinophyceae thecate undet. 1 (>20 μm)	3.12	14.97	2.08	4.00	4.00
Gomphosphaeria aponina Kützing	0.00	10.02	1.70	3.27	7.27
Coscinodiscus spp.	0.00	9.50	1.61	3.08	10.36
Protoperidinium spp.	1.34	9.81	1.59	3.06	13.41
Oscillatoria spp.	2.72	9.54	1.56	3.00	16.41
Rhabdonema adriaticum Kützing 1844	8.84	3.19	1.41	2.71	19.12
Entomoneis alata (Ehrenberg) Ehrenberg 1845	10.34	5.11	1.41	2.70	21.82
Thalassionema spp.	8.89	3.14	1.37	2.62	24.44
Ostreopsis cf. *heptagona*	8.64	3.27	1.36	2.62	27.06
Chaetoceros laevis G. Leuduger-Fortmorel 1892	8.60	2.20	1.34	2.58	29.64
Bleakeleya notata (Grunow) Round	3.27	7.36	1.34	2.57	32.21
Coolia spp.	8.18	3.12	1.29	2.48	34.69
Mastogloia fimbriata (T. Brightwell) Grunow 1863	1.69	7.82	1.29	2.47	37.16
Thalassiophysa hyalina (Grev.) Paddock & P.A. Sims 1981	0.00	7.69	1.28	2.46	39.63
Cyclotella spp.	0.00	6.84	1.25	2.40	42.03
Gonyaulax spp.	1.65	7.53	1.25	2.39	44.42
Synedra cf. *fulgens* var. *gigantea*	5.37	6.53	1.24	2.39	46.81
Chaetoceros curvisetus Cleve 1889	1.26	7.19	1.22	2.35	49.16
Chaetoceros decipiens Cleve 1873	6.60	4.75	1.21	2.32	51.47
Licmophora spp.	7.70	6.12	1.20	2.31	53.78
Cyanophyceae undet. 2f	9.24	3.80	1.20	2.31	56.09
Synedra spp.	5.11	6.61	1.19	2.28	58.37
Prorocentrum belizeanum M.A. Faust 1993	6.66	6.03	1.17	2.25	60.62
Licmophora flabellata (Grev.) C. Agardh 1831	6.48	1.54	1.12	2.15	62.77
Microtabella interrupta (Ehrenberg) Round 1990	11.04	8.24	1.09	2.10	64.87
Navicula transitans Cleve 1883	6.39	0.00	1.08	2.08	66.95
Synedra crotonensis var. *prolongata* Grunow 1881	12.97	8.29	1.06	2.04	68.99
Gambierdiscus spp.	5.22	3.59	1.05	2.02	71.01

The total biovolume values are given as ln ($\mu m^3 L^{-1} + 1$). The average dissimilarity is based on Bray–Curtis similarity and is computed by calculating the dissimilarity between Summer months (June and July) and the Winter months (December and January). The % contribution values indicate how much each taxon contributes to the overall dissimilarities between the two regions, with the cumulative % value summing these values to demonstrate how the overall dissimilarity is built by the contributing species.

and the taxa considered (Fig. 7a). Axis 1 was correlated mainly with 3dw ($r = 0.76$), 3dT ($r = -0.77$) and 3dL ($r = -0.73$), whereas on axis 2, the highest correlation was seen for 3dw ($r = -0.51$). Both axes were statistically significant (Montecarlo testing, $P < 0.001$).

As presented previously, a clear seasonal-spatial structure was apparent in the phytoplankton assemblage over the period of study (Fig. 6b). These differences are explained in terms of how the various taxa relate to the environmental variables in the CCA plot. For example, the upper right panel of the CCA illustrates the winter communities, characterized by species positively linked to 3dw and negatively linked to 3dT. In particular, Bacillariophyta (*C. closterium*, *C. decipiens*, *Chaetoceros laciniosus*, *Chaetoceros laevis*, *Chaetoceros wighamii*, *Chaetoceros* spp., *C. moniligera*, *Entomoneis alata*, *Eunotia* cf. *lunaris*, *H. hauckii*, *Licmophora flabellata*, *Microtabella interrupta*, *Synedra crotonensis* var. *prolongata*, *Striatella unipunctata*, *Navicula* spp., *Tabellaria* cf. *fenestrata*), some flagellates (Cryptophyceae undet. and Phytoflagellates undet.), one Dinophyta (*Gambierdiscus* spp.) and Cyanobacteria (Cyanophycea undet. 2f) taxa best displayed this pattern.

Many of these taxa were also characteristic of the bayside sites, while fewer were associated with the oceanside sites, suggesting the winter signal was stronger at the bayside sites, which is expected given the shallower water and lesser volume of Florida Bay versus the Atlantic Ocean.

The left portion of the CCA displays the summer communities that are characterized by taxa positively linked to 3dT and 3L. In particular, Dinophyta taxa [*Protoperidinium* spp., *Scrippsiella* spp., *T. furca* and Dinophyceae thecate undet. 1 (>20 μm)], four Bacillariophyta (*Coscinodiscus* spp., *Mastogloia fimbriata*, *T. hyalina*, *Toxarium undulatum*) and two Cyanobacteria (*G. aponina*, *Oscillatoria* spp.) displayed these characteristics.

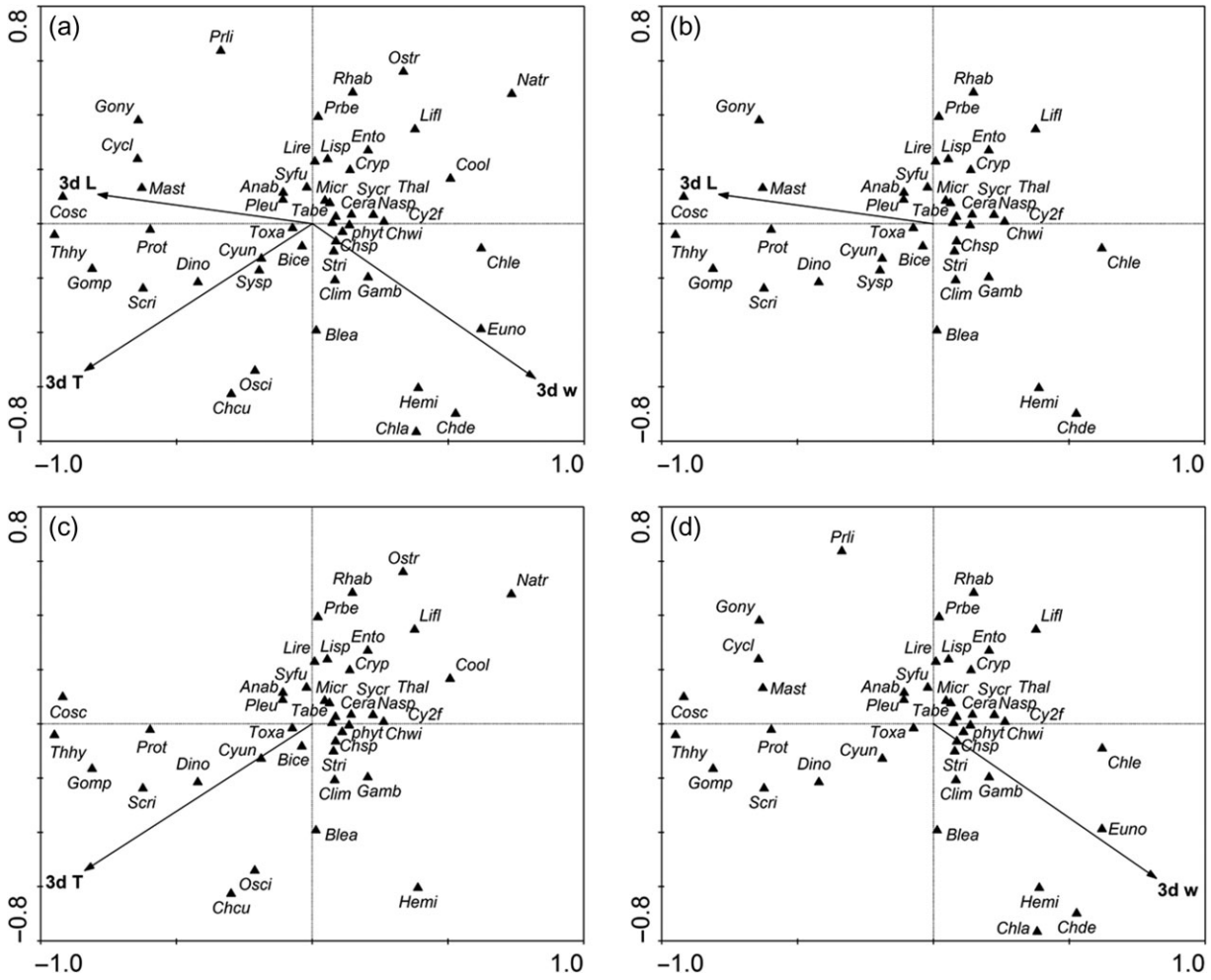

Fig. 7. CCA ordination plots defined by first two axes representing the analysis between phytoplankton taxa and environmental selected variables. Taxa abbreviation, see Table II.

DISCUSSION

This study represents the first in-depth examination of the structure of the phytoplankton community from four distinct ecotypes in the FK, characterized by tropical conditions and different habitat types. The results presented herein expand the knowledge on phytoplankton taxonomy and biodiversity in the region, especially in relation to the varying environmental conditions captured in this study. The phytoplankton community exhibited differences on geographic and seasonal scales, reflecting that the phytoplankton assemblage structure was established and related to regional differences in basic ecosystem characteristics, i.e. "macro-ecological filters" (Vadrucci *et al.*, 2008; Phlips *et al.*, 2010) and seasonality. The results clearly demonstrate the existence of variability of the most important structural characteristics in the community, including composition and biomass. On a global scale, these two key components of phytoplankton structure varied significantly at a higher taxonomic level, demonstrated by the observation that Bacillariophyta were the most representative functional group in diversity and biomass terms, followed by Dinophyta and Cyanobacteria (Appendix I and Table II).

Phytoplankton composition and distribution

From a spatial and temporal perspective, the data analyzed revealed distinct patterns in phytoplankton composition and total biomass. Different taxonomic/functional group dominated phytoplankton communities bayside (HGB and TPH) and oceanside (LKH and TRL) (Fig. 6). This finding indicates that in the same geographic area (e.g. the FK), different regional hydrological, physicochemical and biological characteristics play an important role determining the presence, dominance or co-existence

of different taxa. The wide distribution of phytoplankton species is, therefore, mosaic-like, reflecting the distribution of corresponding habitats (Padisák *et al.*, 2015).

High compositional variability was observed at spatial and temporal scales. The dominance of Bacillariophyta in the four ecotypes indicates that these organisms were not only tolerant of environments characterized by strong vertical mixing energy (Wyatt and Horwood, 1973; Margalef, 1978; Margalef *et al.*, 1979; Smayda and Reynolds, 2001; Badylak and Phlips, 2004), but could also survive in totally opposite conditions (i.e. calm summer waters). This result is because different taxa, even within the same phylum, are often characterized by different adaptive strategies that can permit survival in such extremely variable environmental conditions.

Cyanobacteria were cosmopolitan, but in biomass terms and dimensionally, they dominated in ecotypes that showed a low average wave range, such as TPH and HGB (Figs 6a and 7a). This result demonstrates how water energy can influence cyanobacteria growth, in which they can dominate the phytoplankton community of a flow-restricted environment (Badylak and Phlips, 2004).

Similarly, the success of dinoflagellate species at HGB and LKH is probably due to the low tidal mixing energy that characterizes sheltered ecotypes like HGB, particularly during the summer when wind-mixing energy is at a minimum. Several studies have shown that, in general, motile phytoplankton (including dinoflagellates), are selectively favored in environments where vertical mixing energy is limited, because of their ability to access the resources needed for growth and survival, principally light and nutrients (Margalef, 1978, 1997; Smayda and Reynolds, 2001).

Interestingly, however, *Gambierdiscus* spp. was the most dominant dinoflagellate at LKH (which had a higher average wave height). *Gambierdiscus* is benthic in general, so this finding may be a result of resuspension.

Dynamics of discriminating phytoplankton taxa

The present study supports the existence of a high level of taxonomic heterogeneity among both ecotypes and seasons (Tables III and IV). This heterogeneity can be partially explained by large-scale variations in abiotic factors. Specifically, the inter-ecosystem variability of taxonomic structure can be explained by the geographic position of ecotypes, with those ecotypes that were spatially closer being more similar in their taxonomic structure than ecotypes that were further apart.

The geographic position of an ecotype acts as a filter for the response to climatic variation and consequently affects the patterns of inter- and intra-annual variation of ecosystem variables (Benson *et al.*, 2000; Quinlan *et al.*, 2003; Vadrucci *et al.*, 2008). According to their geographic position, our results confirm the presence of two spatial groups; one belonging to the open ocean (TRL and LKH ecotypes), and the other to Florida Bay (HGB and TPH ecotypes; Fig. 6a). As a result of temporal variation, there are also two seasonal groups characterized by winter and summer taxa (Fig. 6b). This different spatio-temporal grouping may be due to the low wave ranges characteristic of HGB and TPH (Table I), both bayside sites. Opposite conditions characterize the two oceanside sites. Temperature was the most important factor determining the differences at the temporal (seasonal) scale (Fig. 7).

Phytoplankton structural differences (by season and site) were explained by 28 taxa (70% dissimilarity according to ANOSIM; Tables III and IV). In general, this finding could reflect different preferences for environmental conditions in which they can survive, grow and reproduce optimally. Each species is, therefore, largely confined to a specific interval along an environmental gradient. Each species is, thus, presumed to occur in a characteristic, limited range of the multidimensional habitat space and within this, each species tends to be the most abundant around a specific environmental optimum (Jamil *et al.*, 2014).

Phytoplankton and environmental conditions

The composition of phytoplankton expected to be found in any system will be dictated by a number of environmental variables such as nutrient and light availability, salinity and seasonal changes (Fonseca and Bicudo, 2007). Understanding which variables are most dominant for specific ecosystems is necessary for accurately assessing assemblage dynamics (Hack, 2014). Our results are consistent with the role that physical and environmental processes play in determining phytoplankton fluctuations (Smayda, 2002). The phytoplankton were distributed along gradients defined by wave energy, temperature and light intensity (Fig. 7). The placement of the taxa within these gradients reveals (some of) the conditions that influence the success of these taxa, particularly on spatial and seasonal scales. Dinoflagellates were selected by high temperature, high light and low wave energy values, conditions that are typical of summer season and bayside sites (Fig. 7b–d). Some Cyanobacteria occurred in the same environmental conditions. They tend to be favored groups at higher temperatures (Jamil *et al.*, 2014). Increased temperatures induce stronger stratification and shallower mixing depths, resulting in increased light availability for

floating cyanobacteria. High temperatures also have a direct effect on optimizing nitrogen fixation by enhancing the rate of gas diffusion into heterocysts (Bauersachs *et al.*, 2014; Mantzouki *et al.*, 2015). Alternatively, a few diatoms, characterized by elongated shape and different size, are present along this diagonal environmental gradient (Fig. 7c). This may indicate that temperature plays an important role in the aggregations of some species, resulting in higher sinking rates, and removal of other diatoms from the water column (Thorton and Thake, 1998).

Changing light regimes can affect phytoplankton assemblages (Edwards *et al.*, 2015). In general, diatoms are thought to perform relatively well under limiting light and excessive light (Richardson *et al.*, 1983), as well as fluctuating light conditions (Litchman, 1998). Additionally, smaller cells are thought to maintain higher photosynthetic rates under light limitation (Geider *et al.*, 1986; Finkel, 2001) while larger cells may be less susceptible to photoinhibition under excessive light (Key *et al.*, 2010). Diatoms characterized in this study showed high intragroup size and shape variability. For example, various taxa belonging to the same genus and characterized by the same shape (e.g. *C. laevis*, *C. whigamii*, etc.), showed high size variability. These differences may reflect adaptations to varying light conditions. Additionally, those diatoms with elongated and attenuated shapes are able to maximize the surface area exposed to light per unit of volume at low light conditions (Sommer, 1998; Morabito *et al.*, 2007; Stanca *et al.*, 2013a).

Interestingly, nutrient variability was not as influential as the physical parameters in structuring the phytoplankton community. This result could be due to the monthly variability observed in the nutrient data (Fig. 3), or could reflect that the (sub)tropical phytoplankton taxa encountered in this study are adapted to oligotrophic conditions, generally typical of tropical coastal environments (Corredor *et al.* 1999; Souza *et al.*, 2013; Stanca *et al.*, 2013b). With concerns of increasing nutrient loading in many tropical, coastal ecosystems, however, nutrients are likely to have an increasing impact in the future (Lapointe and Clark, 1992).

CONCLUSION

Functional groups within phytoplankton communities can respond differently to environmental conditions, altering their relative abundance. Dinoflagellates and cyanobacteria displayed changes along an environmental gradient consisting of changing light, temperature and wave energy. Diatoms, on the other hand, did not exhibit clear relationships to gradients, possibly reflecting the high diversity within this phylum, including differences in cell shape and size that allows this group as a whole to adapt to many different (but specific environmental regimes).

ACKNOWLEDGEMENTS

We would like to thank Ashley Brandt, Amanda Ellsworth and Alex Leynse for their assistance in the field and laboratory (Florida Gulf Coast University). Special thanks are due to Prof. A. Basset for his encouragement to apply a biodiversity phytoplankton project, extending my phytoplankton knowledge abroad (E.S.).

FUNDING

Funding was provided to E.S. by a post-doc fellowship "Lina Rizzo- per ricerche nel campo della Planctologia" from the Accademia Nazionale dei Lincei (Rome) and to M.L.P. by NOAA NOS (Cooperative Agreements NA11NOS478-0060 and NA11NOS4780028). This is ECOHAB publication number 848.

REFERENCES

Al-Kandari, M., Al-Yamani, F. Y. and Al-Rifaie, K. (2009) *Marine Phytoplankton Atlas of Kuwait's Waters*. Kuwait Institute for Scientific Research, Safat, Kuwait.

Alves-De Souza, C., González, M. T. and Iriarte, J. L. (2008) Functional groups in marine phytoplankton assemblages dominated by diatoms in fjords of southern Chile. *J. Plankton Res.*, **30**, 1233–1243.

Arrigo, K. R. (2005) Marine microorganisms and global nutrient cycles. *Nature*, **437**, 349–355.

Badylak, S. and Phlips, E. J. (2004) Spatial and temporal patterns of phytoplankton composition in a subtropical coastal lagoon, the Indian River Lagoon, Florida, USA. *J. Plankton Res.*, **26**, 1229–1247.

Bauersachs, T., Stal, L. J., Grego, M. and Schwark, L. (2014) Temperature induced changes in the heterocyst glycolipid composition of N-2 fixing heterocystous cyanobacteria. *Org. Geochem.*, **69**, 98–105.

Benson, B. J., Lenters, J. D., Magnuson, J. J., Stubbs, M., Kratz, T. K., Dillon, P. J., Hecky, R. E. and Lathrop, R. C. (2000) Regional coherence of climatic and lake thermal variables of four lake districts in the Upper Great Lake Region of North America. *Freshwater Biol.*, **43**, 517–527.

Bray, R. J. and Curtis, J. T. (1957) An ordination of the upland forest communities of southern Wisconsin. *Ecol. Monogr.*, **27**, 325–349.

Clarke, K. R. and Gorley, R. N. (2015) *PRIMER v7: User Manual/Tutorial*. PRIMER-E, Plymouth, UK.

Clarke, K. R. (1993) Non-parametric multivariate analyses of changes in commmunity structure. *Aust. J. Eco.*, **18**, 117–143.

Corredor, J. E., Howarth, R. W., Twilley, R. R. and Morrell, J. M. (1999) Nitrogen cycling and anthropogenic impact in the tropical Interamerican seas. *Biogeochemisty*, **46**, 163–178.

Cupp, E. E. (1977) *Marine Plankton Diatoms of the West Coast of North America*. Otto Koeltz Science Publishers, Koenigstein.

Dodge, J. D. (1982) *Marine Dinoflagellates of the British Isles*. Her Majesty's Stationery Office, London.

Edwards, K. F., Thomas, M. K., Klausmeier, C. A. and Litchman, E. (2015) Light and growth in marine phytoplankton: allometric, taxonomic, and environmental variation. *Limnol. Oceanogr.*, **60**, 540–552.

Falkowski, P. G., Katz, M. E., Knoll, A. H., Quigg, A., Raven, J. A., Schofield, O. and Taylor, F. J. R. (2004) The evolution of modern eukaryotic phytoplankton. *Science*, **305**, 354–360.

Faust, M. A. and Gullendge, R. A. (2002) *Identifying harmful marine dinoflagellates, Contribution from the United States National Herbarium*, **Vol 42**, Smithsonian Institution, NMNH National Museum of Natural History, Washington, DC, pp. 1–144.

Field, C. B., Behrenfeld, M. J., Randerson, J. T. and Falkowski, P. G. (1998) Primary production of the biosphere: integrating terrestrial and oceanic components. *Science*, **281**, 237–240.

Finkel, Z. V. (2001) Light absorption and size scaling of lightlimited metabolism in marine diatoms. *Limnol. Oceanogr.*, **46**, 86–94.

Foged, N. (1984) Freshwater and Littoral Diatoms from Cuba. *Bibliotheca Diatmol.*, **5**, 1–243 J. Cramer, Berlin.

Fonseca, B. M. and Bicudo, C. E. M. (2007) Phytoplankton Seasonal Variation in a Shallow Stratified Eutrophic Reservoir (Garças Pond, Brazil). *Hydrobiologia*, **600**, 267–282.

Geider, R. J., Platt, T. and Raven, J. A. (1986) Size dependence of growth and photosynthesis in diatoms: a synthesis. *Mar. Ecol. Prog. Ser.*, **30**, 93–104.

Hack B. (2014) Effects of regime shift on phytoplankton community composition in Gunston Cove of the tidal Potomac River. Thesis Bachelor of Science. University of South Carolina.

Harrison, W. G. (1976) Nitrate metabolism of the red tide dinoflagellate *Gonyaulax polyedra* Stein. *J. Exp. Mar. Biol. Ecol.*, **21**, 9–209.

Hein, M. K., Winsborough, B. M. and Sullivan, M. J. (2008) *Bacillariophyta (Diatoms) of the Bahamas Hardcover*. A.R.G. Gantner, Königstein, Germany, Koeltz Scientific Books.

Hillebrand, H., Durselen, C. D., Kirschtel, D., Pollingher, U. and Zohary, T. (1999) Biovolume calculation for pelagic and benthic microalgae. *J. Phycol.*, **35**, 403–424.

Hoppenrath, M., Murray, S. A., Chomérat, N. and Horiguchi, T. (2014) *Marine Benthic Dinoflagellates – Unveiling Their Worldwide Biodiversity*, **276**, Kleine Senckenberg-Reihe, Band 54, Schweizerbart, Stuttgart, Germany.

Iglesias-Rodríguez, M. D., Brown, C. W., Doney, S. C., Kleypas, J., Kolber, D., Kolber, Z., Hayes, P. K. and Falkowski, P. G. (2002) Representing key phytoplankton functional groups in ocean carbon cycle models: Coccolithophorids. *Global Biogeochem. Cycles*, **16**, 1100, 10.1029/2001BG001454.

Jamil, T., Kruk, C. and ter Braak, C. J. F. (2014) A unimodal species response model relating traits to environment with application to phytoplankton communities. *PLoS ONE*, **9**, 1–14.

Key, T., McCarthy, A., Campbell, D. A., Six, C., Roy, S. and Finkel, Z. V. (2010) Cell size trade-offs govern light exploitation strategies in marine phytoplankton. *Environ. Microbiol.*, **12**, 95–104.

Kruk, C., Peeters, E. T. H. M., Van Nes, E. H., Huszar, V. L. M., Costa, L. S. and Scheffer, M. (2011) Phytoplankton community composition can be predicted best in terms of morphological groups. *Limnol. Oceanogr.*, **56**, 110–118.

Lapointe, B. E. and Clark, M. W. (1992) Nutrient inputs from the watershed and coastal eutrophication in the Florida Keys. *Estuaries*, **15**, 465–476.

Le Quéré, C., Harrison, S. P., Colin Prentice, I., Buitenhuis, E. T., Aumont, O., Bopp, L., Claustre, H., Cotrim Da Cunha, L. *et al* (2005) Ecosystem dynamics based on plankton functional types for global ocean biogeochemistry models. *Global Change Biol.*, **11**, 2016–2040.

Litchman, E. (1998) Population and community responses of phytoplankton to fluctuating light. *Oecologia*, **117**, 247–257.

Litchman, E., Klausmeier, C. A., Schofield, O. M. and Falkowski, P. G. (2007) The role of functional traits and trade-offs in structuring phytoplankton communities: scaling from cellular to ecosystem level. *Ecol. Lett.*, **10**, 1170–1181.

Lobban, C. S. and Schefter, M. (2012) Coral-reef diatoms (Bacillariophyta) from Guam: new records and preliminary checklist, with emphasis on epiphytic species from farmer-fish territories. *Micronesica*, **43**, 237–479.

Malviyaa, S., Scalco, E., Audic, S., Vincent, F., Veluchamy, A., Poulain, J., Wincker, P., Daniele Iudicone, D. *et al* (2016) Insights into global diatom distribution and diversity in the world's ocean. *PNAS*, **113**, 1516–1525.

Mantzouki, E., Visser, P. M., Bormans, M. and Ibelings, B. W. (2015) Understanding the key ecological traits of cyanobacteria as a basis for their management and control in changing lakes. *Aquat. Ecol.*, **50**, 333–350.

Margalef, R. (1978) Life-forms of phytoplankton as survival alternatives in an unstable environment. *Oceanol. Acta*, **1**, 493–509.

Margalef, R. (1997) Red tides and ciguatera as successful ways in the evolution and survival of an admirable old phylum. In Reguera, B., Blanco, J., Fernandez, L. and Wyatt, T. (eds), Harmful Algae. Proceedings of the VIII International Conference on harmful algae, Vigo, Spain, June 25–29, 1997, pp. 3–7.

Margalef, R., Estrada, M. and Blasco, D. (1979) Functional morphology of organisms involved in red tide as adapting to decaying turbulence. In Taylor, D. L. and Seliger, H. H. (eds), *Toxic Dinoflagellate Blooms*. Elsevier, New York, pp. 89–94.

Morabito, G., Oggioni, A., Caravati, E. and Panzani, P. (2007) Seasonal morphological plasticity of phytoplankton in Lago Maggiore (N. Italy). *Hydrobiologia*, **578**, 47–57.

Olsson, P. and Granelli, E. (1991) Observations on diurnal vertical migration and phased cell division for three coexisting marine dinoflagellates. *J. Plankton Res.*, **13**, 1313–1324.

Nuttle, W. K., and Fletcher P. J. (eds.). 2013. Integrated conceptual ecosystem model development for the Florida Keys/Dry Tortugas coastal marine ecosystem. NOAA Technical Memorandum, OAR-AOML-101 and NOS-NCCOS-161. Miami, Florida. 91 pp.

Paasche, E., Bryceson, I. and Tangen, K. (1984) Interspecific variation in dark nitrogen uptake by dinoflagellates. *J. Phycol.*, **20**, 394–401.

Paerl, H. W. and Huisman, J. (2009) Minireview climate change: a catalyst for global expansion of harmful cyanobacterial blooms. *Environ. Microbiol. Rep.*, **1**, 27–37.

Padisák, J., Vasas, G. and Borics, G. (2015) Phycogeography of freshwater phytoplankton: traditional knowledge and new molecular tools. *Hydrobiologia*, **764**, 3–27.

Patrick, R. M. and Reimer, C. W. (1966) The Diatoms of theUnited States Exclusive of Alaska and Hawaii. Monographs of the Academy of Natural Sciences of Philadelphia, **1**, 688 pp., 64 pls.

Pena, M. A. (2003) Plankton size classes, functional groups and ecosystem dynamics: an introduction. *Progr. Oceanogr.*, **57**, 239–242.

Phlips, E. J., Badylak, S., Christman, M. C. and Lasi, M. A. (2010) Climatic Trends and Temporal Patterns of Phytoplankton Composition, Abundance, and Succession in the Indian River Lagoon, Florida, USA. *Estuaries Coasts*, **33**, 498–512.

Quinlan, R., Paterson, A. M., Hall, R. I., Dillon, P. J., Wilkinson, A. N., Cummins, B. F., Douglas, M. S. V. and Smol, J. P. (2003) A landscape approach to examining spatial patterns of limnological variables and long term environmental change in a Southern Canadian Lake district. *Freshwater Biol.*, **48**, 1676–1697.

Richardson, K., Beardall, J. and Raven, J. A. (1983) Adaptation of unicellular algae to irradiance: an analysis of strategies. *New. Phytol.*, **93**, 157–191.

Roselli, L. and Basset, A. (2015) Decoding size distribution patterns in marine and transitional water phytoplankton: from community to species level. *PLoS One*, **10**, e0127193.

Sciandra, A. (1991) Coupling and uncoupling between nitrate uptake and growth rate in *Prorocentrum minimum* under different frequencies of pulsed nitrate supply. *Mar. Ecol. Prog. Ser.*, **72**, 261–269.

Smayda, T. J. and Reynolds, C. S. (2001) Community assembly in marine phytoplankton: application of recent models to harmful dinoflagellate blooms. *J. Plankton Res.*, **23**, 447–461.

Smayda, T. J. and Reynolds, C. S. (2003) Strategies of marine dinoflagellate survival and some rules of assembly. *J. Sea Res.*, **49**, 95–106.

Smayda, T. J. (2002) Turbulence, watermass stratification and harmful algal blooms: an alternative view and frontal zones as "pelagic seed banks". *Harmful Algae*, **1**, 95–112.

Sommer, U. (1998) Silicate and the functional geometry of marine phytoplankton. *J. Plankton Res.*, **20**, 1853–1859.

Sournia, A. (1986) Atlas du phytoplancton marin. *Introduction, Cyanophycees, Dictyochophycees, Dinophycees, et Raphidophycees*, **Vol. 1**, Centre National de la Recherche Scientifique, Paris, pp. 1–219.

Souza, J. S. D., Stanca, E., Roselli, L., Attayde, J. L., Panosso, R. and Basset, A. (2013) A checklist of phytoplankton species around the Equator in Guaraíras, Galinhos and Diogo Lopes lagoons (Rio Grande do Norte, Brazil). *Transit. Water. Bull.*, **7**, 220–232.

Sun, J. and Liu, D. Y. (2003) Geometric models for calculating cell biovolume and surface area for phytoplankton. *J. Plankton Res.*, **25**, 1331–1346.

Stanca, E., Cellamare, M. and Basset, A. (2013a) Geometric shape as a trait to study phytoplankton distributions in aquatic ecosystems. *Hydrobiologia*, **701**, 99–116.

Stanca, E., Roselli, L., Cellamare, M. and Basset, A. (2013b) Phytoplankton composition in the coastal Magnetic Island lagoon, Western Pacific Ocean (Australia). *Transit. Water. Bull.*, **7**, 145–158.

Ter Braak, C. J. F. (1986) Canonical correspondence analysis: a new eigenvector technique for multivariate direct gradient analysis. *Ecology*, **67**, 1167–1179.

Thorton, D. C. O. and Thake, B. (1998) Effect of temperature on the aggregation of Skeletonema costatum (Bacillariophyceae) and the implication for carbon flux in coastal waters. *Mar. Ecol. Prog. Ser.*, **174**, 223–231.

Tomas, R. C. (1997) *Identifying Marine Phytoplankton*. Academic Press, St. Petersburg.

Trobajo Pujadas, R. (2007) Ecological analysis of periphytic diatoms in Mediterranean coastal wetlands (Empordà wetlands, NE Spain). In Witkowski, A. (ed.), *Diatom Monographs*, **Vol. 7**, Gantner Verlag, Ruggell, p. 210.

Vadrucci, M. R., Cabrini, M. and Basset, A. (2007) Biovolume determination of phytoplankton guilds in transitional water ecosystems of Mediterranean Ecoregion. *Transit. Water. Bull.*, **2**, 83–102.

Vadrucci, M. R., Sabetta, L., Fiocca, A., Mazziotti, C., Silvestri, C., Cabrini, M., Guardiani, B., Konjka, E. *et al* (2008) Statistical evaluation of differences in phytoplankton richness and abundance as constrained by environmental drivers in transitional waters of the Mediterranean basin. *Aquatic Conserv Mar. Freshw. Ecosyst.*, **18**, 88–104.

Witkowski, A., Lange Bertalot, H. and Metzeltin, D. (2000) Diatom flora of marine coasts I. In LangeBertalot, H. (ed.), *Annotated diatom micrographs. Iconographia Diatomologica*, **7**, A. R. G. GantnerVerlag, Königstein, Germany, 925, Diversity-Taxonomy-Identification.

Wyatt, T. and Horwood, J. (1973) A model which generates red tides. *Nature*, **244**, 238–240.

Zhang, H. Y., Ludsin, S. A., Mason, D. M., Adamack, A. T., Brandt, S. B., Zhang, X. S., Kimmel, D. G., Roman, M. R. *et al* (2009) Hypoxia-driven changes in the behavior and spatial distribution of pelagic fish and mesozooplankton in the northern Gulf of Mexico. *J. Exp. Mar. Biol. Ecol.*, **381**, S80–S91.

WEB REFERENCES

http://phytobioimaging.unisalento.it/en-us/products/AtlasOfShapes.aspx?ID_Tipo=0
http://windguru.cz/int/; GFS 27 km daily archive; Islamorada, FL
http://www.ncdc.noaa.gov
https://westerndiatoms.colorado.edu/taxa
http://botany.si.edu/references/dinoflag/intro.htm

APPENDIX

Appendix I: List of phytoplankton taxa identified in the four ecosystems studied.

Taxon	HGB	LKH	TPH	TRL
Bacillariophyta				
Bacillariophyceae				
Amphiprora spp.	X		X	
Amphora cf. *hyalina*				X
Amphora spp.	X	X		
Auricula complexa (Gregory) Cleve				X
Bacillaria paxillifera (O.F.Müller) T. Marsson 1901	X	X		
Campylodiscus cf. *limbatus*			X	
Campylodiscus spp.	X			
Entomoneis alata (Ehrenberg) Ehrenberg 1845	X	X	X	X
Eunotia cf. *lunaris*		X	X	X
Gyrosigma spp.		X		
Mastogloia fimbriata (T. Brightwell) Grunow 1863	X	X	X	
Mastogloia spp.	X			
Navicula transitans Cleve 1883	X		X	X
Navicula spp. 9	X			
Navicula spp.	X	X	X	X
Nitzschia sigma (Kützing) W. Smith 1853	X		X	
Pleurosigma spp.	X	X	X	
Pseudo-nitzschia spp.		X		X
Stauroneis legumen (Ehrenberg) Kützing 1844			X	
Surirella spp.	X	X		
Thalassiophysa hyalina (Greville) Paddock & P.A. Sims 1981	X		X	X
Coscinodiscophyceae				
Actinocyclus spp.			X	
Biddulphiopsis titiana (Grunow)von Stosch & R.Simonsen			X	
Coscinodiscus cf. *granii*			X	
Coscinodiscus spp.	X	X	X	
Guinardia striata (Stolterfoth) Hasle in Hasle & Syvertsen 1996				X
Melosira moniliformis (O.F. Müller) C.Agardh 1824	X			
Proboscia alata (Brightwell) Sundström 1986				X
Rhizosolenia imbricata Brightwell 1858				X
Fragilariophyceae				
Bleakeleya notata (Grunow) Round		X	X	X
Ceratoneis closterium Ehrenberg 1839	X	X	X	X
Grammatophora marina (Lyngbye) Kützing 1844	X		X	X
Grammatophora spp.			X	
Licmophora flabellata (Grev.) C. Agardh 1831	X	X	X	X
Licmophora normanniana (Greville 1862) Wahrer 1985	X		X	
Licmophora remulus Grunow 1867	X	X		
Licmophora spp. 1	X		X	
Licmophora spp.	X	X	X	X
Microtabella interrupta (Ehrenberg) Round 1990	X	X	X	X
Podocystis spp.				X
Rhabdonema adriaticum Kützing 1844	X	X	X	
Striatella unipunctata (Lyngbye) C. Agardh 1832	X	X	X	X
Synedra cf. *baculus*	X			
Synedra cf. *fulgens var gigantea*	X	X	X	X
Synedra cf. *superba*	X		X	
Synedra crotonensis var. prolongata Grunow 1881	X	X	X	X
Synedra spp.	X	X	X	X
Tabellaria cf. *fenestrata*	X	X	X	X
Thalassionema spp.	X	X	X	X
Mediophyceae				
Bacteriastrum delicatulum Cleve 1897		X		X
Bacteriastrum spp.				X
Biddulphia biddulphiana (J.E.Smith) Boyer 1900				X
Chaetoceros affinis Lauder 1864	X			

Continued

Appendix I: Continued

Taxon	HGB	LKH	TPH	TRL
Bacillariophyta				
Mediophyceae				
Chaetoceros compressus Lauder 1864				X
Chaetoceros curvisetus Cleve 1889	X	X		X
Chaetoceros danicus Cleve 1889	X			
Chaetoceros decipiens Cleve 1873		X		X
Chaetoceros didymus Ehrenberg 1845			X	X
Chaetoceros laciniosus F. Schütt 1895		X	X	X
Chaetoceros laevis G.Leuduger-Fortmorel 1892	X	X	X	X
Chaetoceros lorenzianus Grunow 1863				X
Chaetoceros peruvianus Brightwell 1856				X
Chaetoceros tenuissimus Meunier 1913			X	X
Chaetoceros tetrastichon Cleve 1897				X
Chaetoceros wighamii Brightwell 1856	X	X	X	X
Chaetoceros spp.	X	X	X	X
Climacosphenia moniligera Ehrenberg	X			X
Cyclotella spp.	X	X	X	X
Cymatosira spp.		X		X
Hemiaulus hauckii Grunow ex Van Heurck 1882				X
Hemiaulus membranaceus Cleve				X
Isthmia enervis Ehrenberg 1838				X
Toxarium undulatum J.W.Bailey 1854	X		X	X
Bacillariophyceae centrales undet.			X	
Bacillariophyceae pennales undet.				X
Chlorophyta				
Pyramimonadophyceae				
Pyramimonas spp.	X		X	
Trebouxiophyceae				
Oocystis spp.			X	
Cryptophyta				
Cryptophyceae				
Cryptophyceae undet.	X	X	X	X
Cyanobacteria				
Cyanophyceae				
Anabaena spp.	X		X	X
Chroococcus spp.	X		X	X
Gomphosphaeria aponina Kützing	X	X	X	
Merismopedia spp.	X		X	
Oscillatoria spp.	X	X	X	X
Spirulina spp.			X	X
Cyanophyceae undet. 2f	X	X	X	X
Cyanophyceae undet. 3f			X	
Cyanophyceae undet.	X	X	X	X
Dinophyta				
Dinophyceae				
Akashiwo sanguinea (K. Hirasaka) G.Hansen & Ø.Moestrup 2000	X			
Amylax triacantha (Jörgensen) Sournia 1984	X			
Ceratium massiliense (Gourret) Karsten 1906				X
Ceratium teres Kofoid 1907				X
Coolia cf. *monotis*			X	
Coolia spp.	X	X	X	X
Dinophysis saccula Stein 1883	X	X		
Gambierdiscus spp.	X	X	X	X
Goniodoma spp.	X	X	X	
Gonyaulax cf. *digitalis*			X	
Gonyaulax polygramma Stein 1883			X	
Gonyaulax scrippsae Kofoid 1911			X	
Gonyaulax spinifera (Claparède & Lachmann) Diesing 1866	X			
Gonyaulax spp.	X	X	X	
Gymnodinium spp.	X			
Heterocapsa cf. *rotundata*		X		
Heterocapsa cf. *psammophila*				X
Heterocapsa niei (Loeblich III) Morrill & Loeblich III 1981		X		
Heterocapsa spp.	X		X	

Continued

Appendix I: Continued

Taxon	HGB	LKH	TPH	TRL
Dinophyta				
Dinophyceae				
Ostreopsis cf. *heptagona*	X	X	X	
Phalacroma rotundatum (Claparéde & Lachmann) Kofoid & Michener 1911				X
Podolampas palmipes Stein 1883				X
Prorocentrum belizeanum M.A. Faust 1993	X	X	X	X
Prorocentrum concavum Y. Fukuyo 1981			X	
Prorocentrum cordatum (Ostenfeld) Dodge 1975	X	X		X
Prorocentrum lima (Ehrenberg) F. Stein 1878	X		X	
Prorocentrum mexicanum Osorio-Tafall 1942			X	X
Prorocentrum scutellum Schröder 1900	X		X	
Prorocentrum spp.		X	X	
Protoperidinium bipes (Paulsen) Balech 1974		X		
Protoperidinium cf. *brochii*				X
Protoperidinium cf. *divergens*	X			
Protoperidinium steinii (Jorgensen) Balech 1974				X
Protoperidinium spp.	X	X	X	X
Scrippsiella spp.	X	X	X	X
Sinophysis microcephalus D.Nie & C.-C.Wang 1944	X			
Tripos furca (Ehrenberg) Vanhoeffen 1897	X	X	X	X
Dinophyceae thecate undet. 1 (>20 μm)	X	X	X	X
Other Phytoplankton				
Other Phytoplankton				
Phytoflagellates undet.	X	X	X	X

The "cf." qualifier was used to indicate specimen that were similar to (or may actually be) the nominate species. Taxa which contain the "undet." (undetermined) identifier were likely to be algal entities, but could not be identified as any known genus. In some cases, species were classified into separate taxa based on size (e.g. Dinophyceae undet. >20 μm). The term "Other" is referred to the group consisting of small phytoflagellates and other undetermined phytoplankton. During phytoplankton identification, sometimes it is not possible to identify the organism to the species level, despite recognizing common characteristics within a group of cells belonging to the same genus. In such cases, to identify that organism is reported as the name of the genus followed by numbered "sp." (e.g. *Oscillatoria* sp. 1, *Oscillatoria* sp. 2, *Oscillatoria* sp. 3, etc.).